



Exploring Wingtip Columnar Vortex Generators for UAV Performance Enhancement

R. Bardera^{1*}, A.A. Rodríguez-Sevillano²⁺, J.C. Matías^{3*}, E. Barroso^{4*}, M. Ojeda⁵⁺, and J.
Fernández⁶⁺

**Instituto Nacional de Técnica Aeroespacial (INTA), Torrejón de Ardoz, Madrid, 28850, Spain*

+Escuela Técnica Superior de Ingeniería Aeronáutica y del Espacio (ETSIAE-UPM), Madrid, 28040, Spain

Abstract:

Efficient aerial vehicle operations depend on minimizing fuel consumption and enhancing aerodynamic efficiency. In pursuit of these goals, the development of wingtip devices has emerged as a viable solution. Leveraging insights from prior studies, this paper investigates the use of innovative wingtip device prototypes based on the passive flow control technology of Columnar Vortex Generators (CVGs) to improve the operational capabilities of Unmanned Aerial Vehicles (UAVs). Three different wingtip device configurations were designed and tested in the wind tunnel of the National Institute for Aerospace Technology (INTA) to examine their aerodynamic efficiency through Particle Image Velocimetry (PIV) measurements. Finally, a comparative analysis of the results is presented, to demonstrate the benefits offered by each wingtip device, facilitating a comprehensive understanding of their relative advantage.

1. Introduction

In recent years, Unmanned Aerial Vehicles (UAVs) have experienced a significant increase in usage across various fields and sectors, owing to their versatility and wide range of applications. These applications are especially valuable for tasks that present risks to manned aircraft and their crews, such as surveillance in hazardous environments, search and rescue missions, and agricultural monitoring.

¹ PhD Aerospace Engineering, Experimental Aerodynamics, barderar@inta.es

² Professor, Flight Mechanics, angel.rodriquez.sevillano@upm.es

³ PhD Aerospace Engineering, Experimental Aerodynamics, matiasgic@inta.es

⁴ PhD Aerospace Engineering, Experimental Aerodynamics, barrosobe@inta.es

⁵ Aerospace Engineering, m.ojedagir@gmail.com

⁶ Aerospace Engineering, jaime.fernandez.anton@alumnos.upm.es

As UAVs are increasingly relied upon for extended operations, ensuring their autonomy becomes critically important. One of the key factors in achieving this autonomy is the reduction of aerodynamic drag, which directly impacts the efficiency and endurance of these vehicles. By minimizing drag, UAVs can achieve longer flight durations, greater fuel efficiency, and improved overall performance, making them more effective and reliable for their intended purposes.

One significant source of aerodynamic drag in wings with finite span is the formation of wingtip vortices, which occur due to the generation of lift on the wing. Because of the pressure difference between the intrados (high-pressure zone) and the extrados (low-pressure zone), a lift force is generated. The pressure differential causes the area of higher pressure to displace the flow from the upper surface, leading to the creation of a vortex. The vortex disturbs the airflow, leading to the emergence of an induced velocity component that creates a local relative flow. This generates an additional induced angle of attack, resulting in an increased drag known as lift-induced drag.

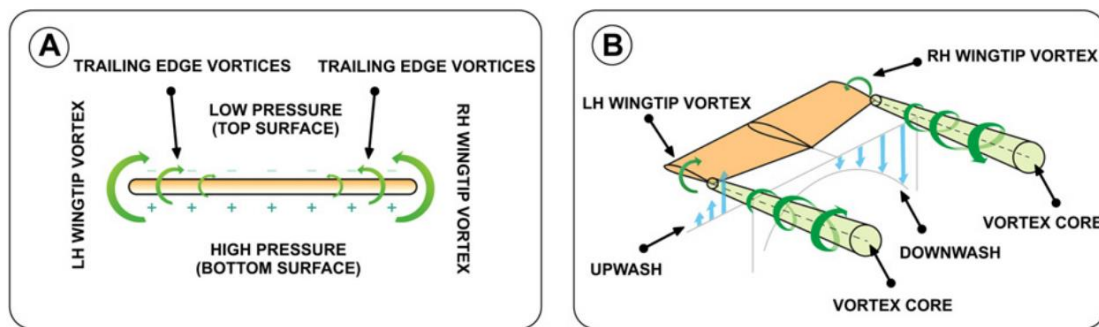


Fig. 1: (A) Pressure differential (B) Wingtip vortices formation [2].

To address this, reducing the length of the vortex is crucial to minimize interference with vehicles or nearby elements that could be affected by the wake, especially considering UAVs, which must be compatible with operations in diverse situations and scenarios. Evidence has demonstrated that wingtip devices effectively reduce lift-induced drag, either by managing to reduce the intensity of the vortex or by deviating the vortex away from the longitudinal axis of the aircraft. By implementing such wingtip devices, UAVs can further enhance their aerodynamic efficiency, thereby extending their operational capabilities and mission effectiveness.

Research and development efforts are therefore focused on innovative designs and technologies that enhance aerodynamic performance. These efforts include advanced materials, streamlined shapes, and sophisticated control systems that together contribute to the UAVs' ability to operate autonomously over extended periods.

In this context, given the favourable outcomes of passive control devices in flow direction, especially the Columnar Vortex Generator [5], a spiral wingtip design was conceptualized with two goals: to decrease vortex intensity, following classical design

principles outlined in previous studies [6]; and to achieve vortex deviation in accordance with CVG placement.

2. Wingtip Devices

Wing model

A literature review investigating wing profiles aimed at mitigating wingtip vortex is conducted, considering studies conducted under conditions similar to the present research [3, 7 - 8]. Based on the outcomes of these studies, the NACA2412 airfoil is chosen for this investigation.

As the main objective is to compare three wingtip device configurations, a simple rectangular wing composed of NACA2412 airfoils is selected. The aerodynamic features of the wing are presented in Table 1 (untwisted, untapered, and straight wing configuration). The aspect ratio (AR) stands at 6.67 which has been selected according to [9], leading to an 800 mm wingspan (b).

Table.1 Aerodynamic features of the simple wing.

Airfoil	c (mm)	b (mm)	AR	S (mm ²)	Θ (°)	Γ (°)	Sweep(°)	λ
NACA 2412	120	800	6.67	96000	0	0	0	1

Passive Flow Control by Columnar Vortex Generator (CVG)

To counteract adverse aerodynamic effects resulting from pressure differentials over the wing, the passive flow control device proposed in this paper is based on the Columnar Vortex Generator (CVG) technology.

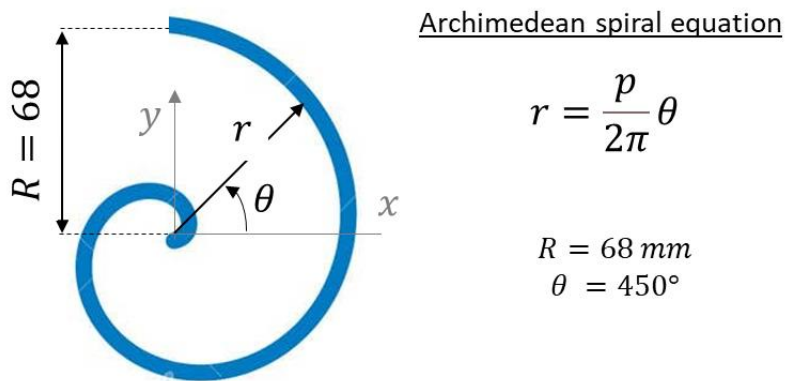


Fig.2 Archimedean spiral parameters.

The CVG device is widely operated in civil [10] or naval applications [5]. It is usually used to control the incoming flow tangentially to the axis of the device. However, in the prototypes of this paper, the main component of the incident flow velocity will be perpendicular to the plane of the spiral; while the velocity component due to pressure differential will be tangential to it. Consequently, the main objective of this work is to

analyze the performance of the devices in this scenario and their capability to reduce induced drag, which will result in a novel alternative to commonly developed wingtip devices. Additionally, its directed flow control capability could offer advantages in certain applications.

Wingtip configurations

The proposed devices to reduce wingtip vortex are designed based on the Columnar Vortex Generator (CVG) geometry, employing an Archimedean spiral configuration. The implementation of these winglets results in an extended wingspan (b) without increasing the lift surface due to the design's specific characteristics. Consequently, the increase in aspect ratio (AR) resulting from the addition of the wingtip does not impact the circulation distribution [11].

All wingtip configurations are constructed as a flat plate profile with a 2 mm thickness, conforming to predetermined parameters for consistency between them (see Figure 2). These geometrical parameters were selected based on their alignment with optimized height [6] and span [12] parameters studied in other winglet designs. Consequently, the ending radius is equal to $R = 68$ mm and the rotated angle is $\theta = 450^\circ$. These parameters prioritize height optimization to avoid overly slender devices, which could compromise both aerodynamic efficiency and structural integrity, considering the challenges associated with adjusting the geometry itself.

According to these requirements, the following three wingtip configurations are designed as: a wingtip device with a clockwise upward spiral CVG, renamed as “Upward CVG”; a counter-clockwise centered spiral device with its center aligned with the midline of the profile, that will be called “Centered CVG”; and a counter-clockwise downward spiral CVG device, “Downward CVG”. Figure 3 shows the three wingtip configurations.

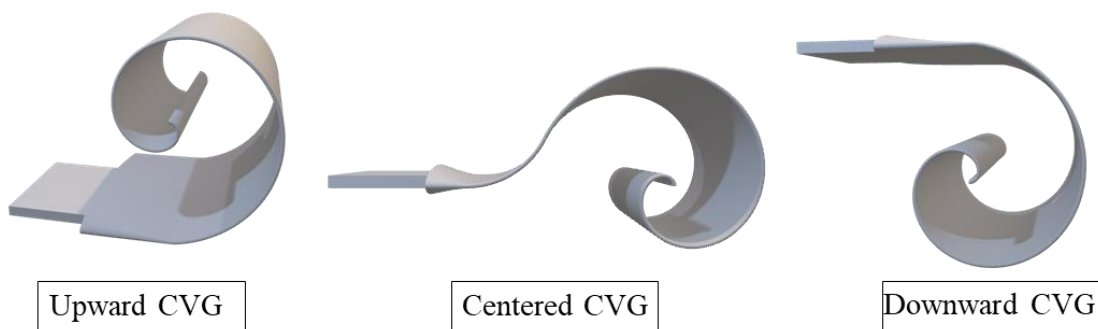


Fig. 3 3D wingtip devices based on the Columnar Vortex Generators (CVG).

3. Experimental set-up

Wind tunnel

The experimental tests were carried out in a low speed wind tunnel nº1 at Instituto Nacional de Técnica Aeroespacial (INTA) in Madrid, Spain. This wind tunnel has an open

elliptical test section of $2 \times 3 \text{ m}^2$. The maximum airflow velocity reaches 60 m/s with a low turbulence intensity of less than 0.5 %. The system is powered by a 450 kW engine operating at 420 V, located on the opposite side of the open test section. Additionally, this wind tunnel features a moving platform that can be adjusted for each experimental test. It is designed with streamlined trailing and leading edges to minimize any potential airflow interference with the flow field during the tests.

Particle Image Velocimetry (PIV)

The experimental analysis of the flow was conducted using Particle Image Velocimetry (PIV). This is a non-intrusive method for measuring flow velocity by analyzing pairs of flow images. Figure 4 shows the main components of this technique.

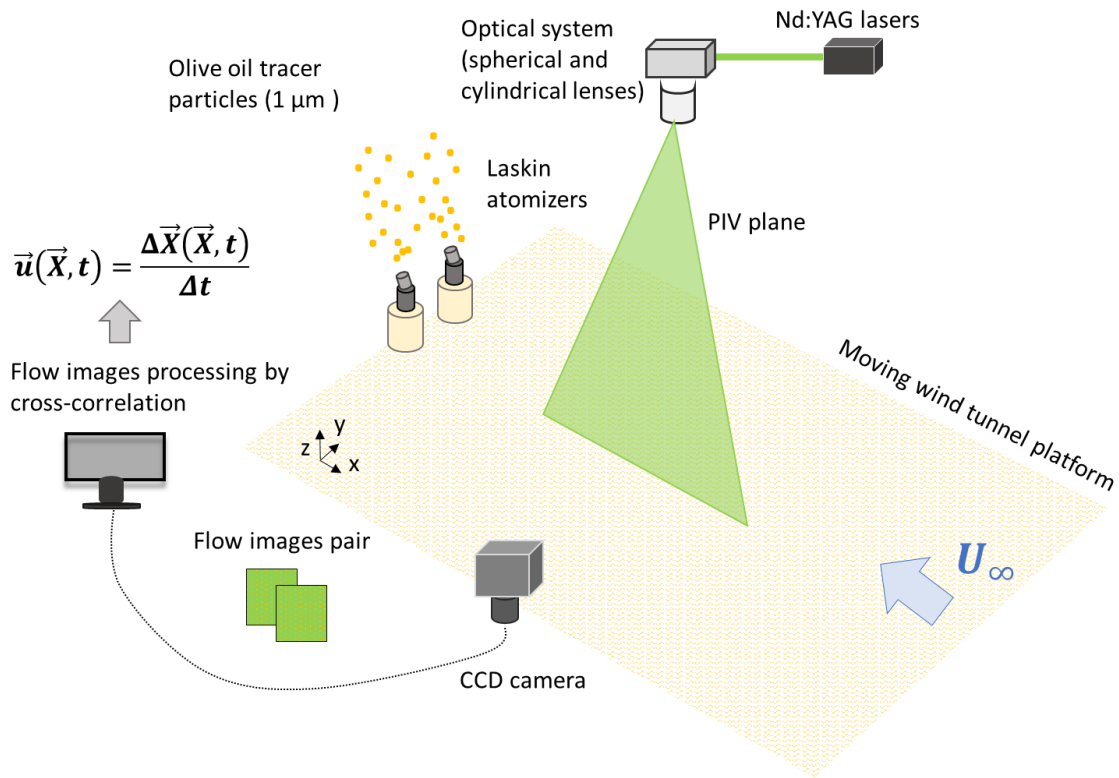


Fig. 4 PIV technique.

In this setup, olive oil tracer particles generated by Laskin atomizers with diameters of 1 μm were seeded in the airflow. A PIV laser plane was generated using two Neodymium-doped Yttrium Aluminium Garnet (Nd) lasers, connected to a system of spherical and cylindrical lenses and the tracer particles were illuminated in the testing section of the wind tunnel. Each laser pulse had an energy of 190 mJ, and the time interval between the pulses was 25 μs. A high-resolution Charged-Coupled Device (CCD) camera, with a resolution of 2048 x 2048 pixels and equipped with a Nikon Nikkor 50 mm 1:1.4D lens, captured the displacement of the tracer particles. The flow images were divided into interrogation windows of 32 x 32 pixels, and the average displacement of the tracer

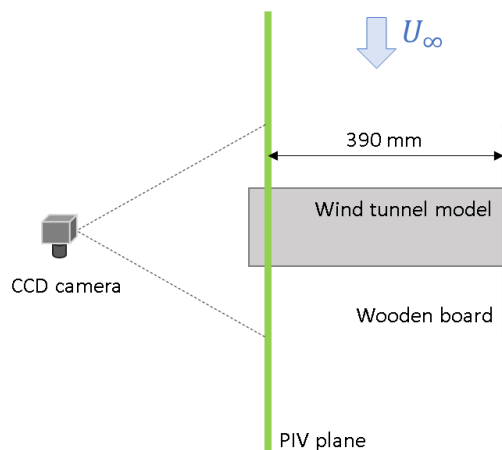
particles in each window was determined using a cross-correlation method implemented with a Fast Fourier Transform (FFT). To meet the Nyquist Sampling Criteria, each interrogation window overlapped by 50%. The correlation peak was refined to subpixel accuracy using a Gaussian curve. Additionally, a local mean filter, based on neighboring windows of 3x3 pixels, was applied to remove spurious vectors.

Experimental set-up

The flow analysis was conducted using two PIV vertical planes: the one referred as lateral plane (see Figure 5) parallel to the freestream velocity of the wind tunnel (U_∞) and the one called as transversal plane, perpendicular to the freestream velocity.

The transversal plane is placed at 390 mm from the wing's junction to obtain a global flow visualization of the wingtip vortex while the lateral plane is located 120 mm downstream of the trailing edge of the wing.

Lateral PIV planes



Transversal PIV planes

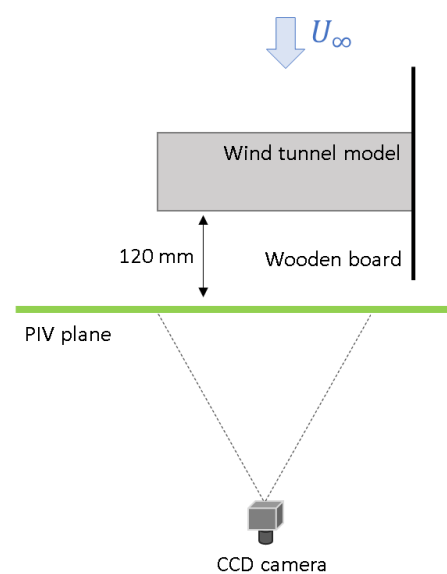


Fig. 5 Location of the PIV planes.

These PIV planes were obtained for the four wing configurations: wing without a wingtip device, wing with an Upward CVG wingtip, wing with a Downward CVG wingtip, and wing with a Centered CVG wingtip; (see Figure 6).

Two flight conditions were analyzed with all wing configurations: one corresponding to cruise flight and the other to takeoff. For the cruise flight condition, it is shown that the wingtip vortex does not establish a stable and formed structure until an angle of attack of 5° [16], so this value is chosen for the test. In the takeoff situation, the objective is to recreate conditions resembling a possible constraint during UAV takeoff operations which involves considering a high angle of attack while also addressing concerns

regarding the onset of stall. The chosen angle is 18° as it is just before the NACA 2412 airfoil enters a stall regime [17]. Finally, a total of 16 cases were analyzed.

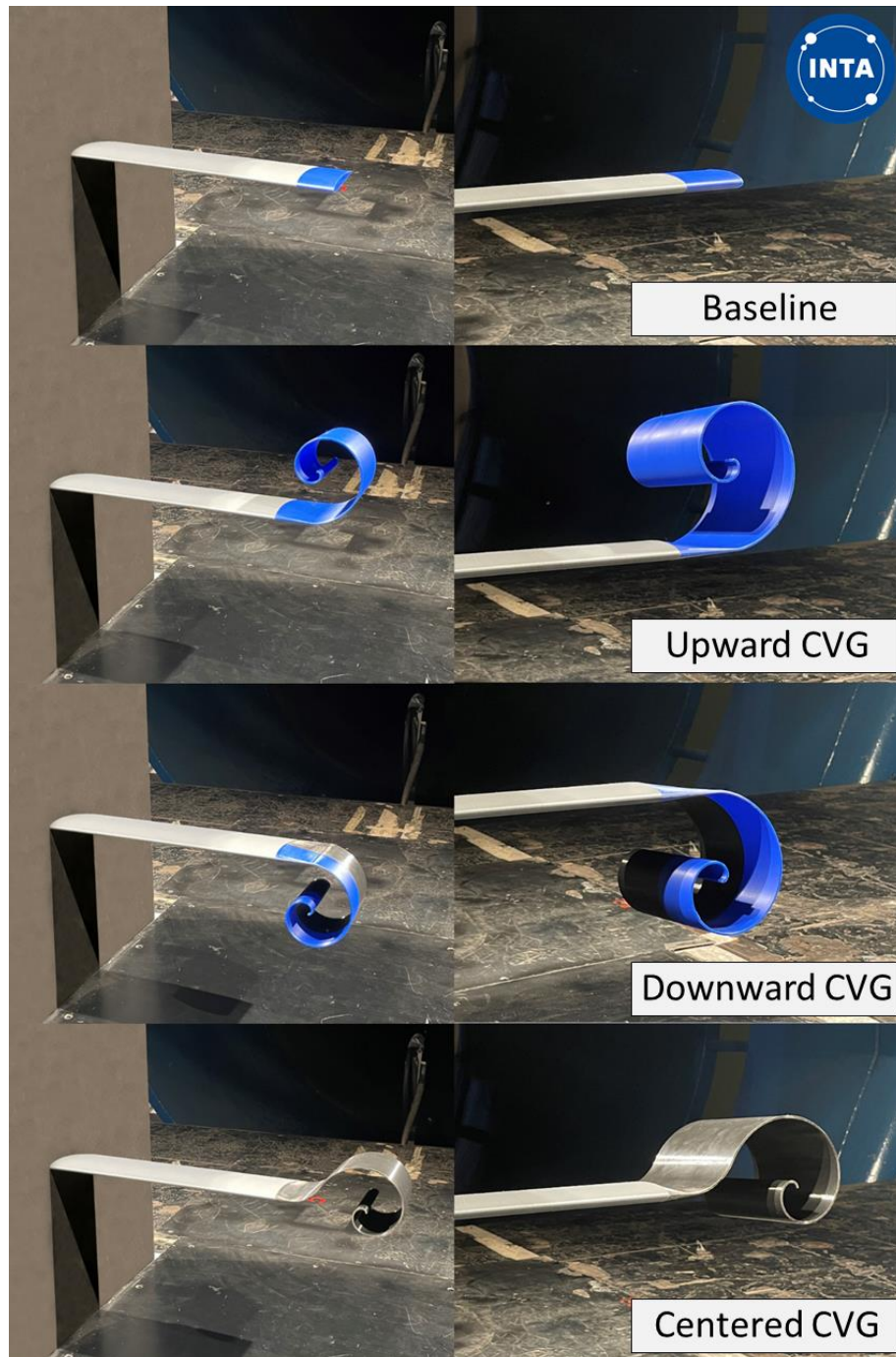


Fig. 6 Wingtip configurations in the wind tunnel.

The experimental tests were conducted with a freestream velocity of the wind tunnel of $U_\infty = 10$ m/s which corresponds to a Reynolds number based on the wing chord of $Re = 8 \cdot 10^4$.

The wind tunnel models were manufactured by 3D printing at INTA. PLA (Polylactic Acid) was selected as additive material due to its high properties for wind tunnel testing.

Due to the wing symmetry, only model halves were tested. The models were placed on the wind tunnel platform using a wooden board as in Figure 6. The wing was positioned at a height of 300 mm to avoid potential ground effects. The variation of the angle of attack was achieved by a threaded rod inserted along the wingspan. The wooden board and the wind tunnel models were painted in black to avoid possible laser reflections during the tests.

4. Experimental results

PIV Velocity maps

Figure 7 shows the non-dimensional velocity maps obtained by PIV at the angle of attack of 5° for the four winglet configurations. The streamlines plotted on the maps shows the flow direction in each case. All wingtip devices effectively reduce the induced velocities from the wingtip vortex, with the downward CVG device achieving the most significant reduction.

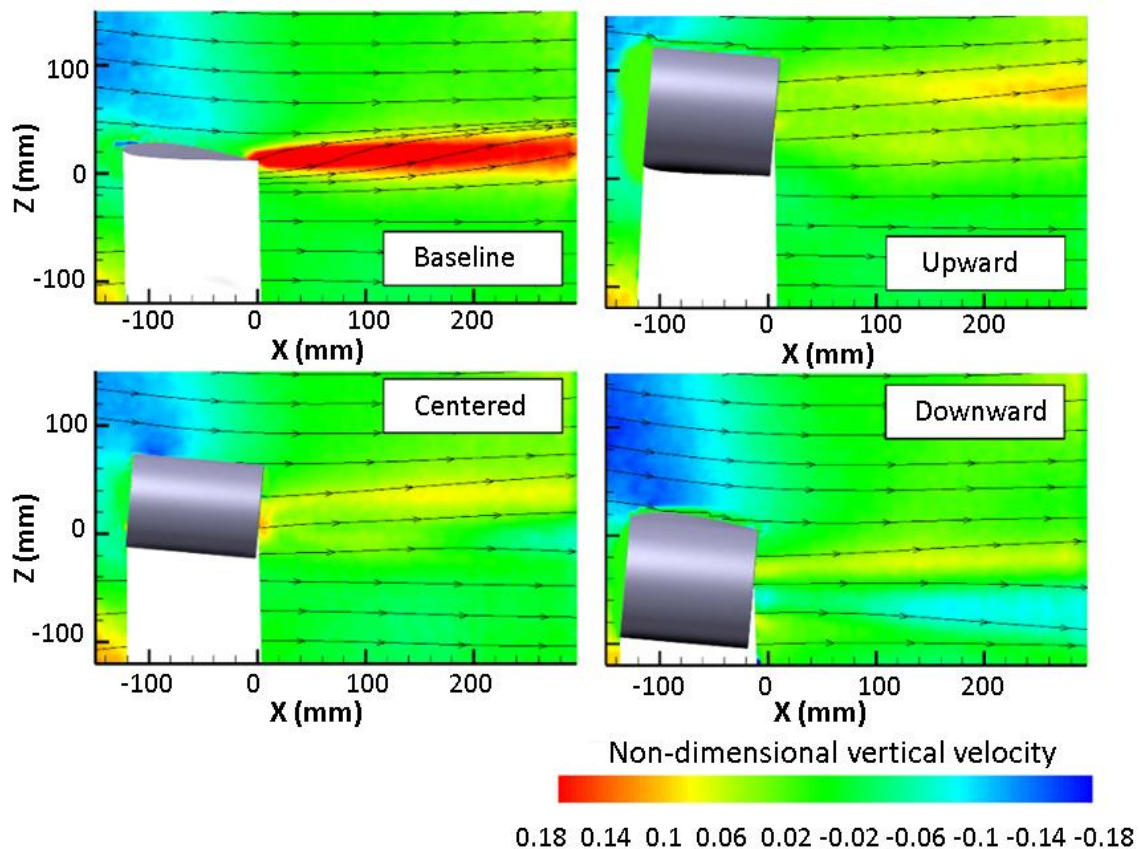


Fig. 7 Comparison of wingtip vortex lateral maps for $\alpha = 5^\circ$.

Figure 8 reveals a transition from a vortex with a distinct core in the baseline configuration to a more diffuse wingtip vortex with a less defined core in the rest

configurations. The cross-sectional maps demonstrate how the flow conforms to the spiral's morphology, resulting in a vortex that deviates from its circular shape. For the centered CVG and downward CVG devices with a "Counterclockwise" spiral, it is observed that the spiral's direction opposes the rotation of the wingtip vortices, leading to a more complex downstream flow region. However, in the upward configuration the vortex flow follows the spiral's direction.

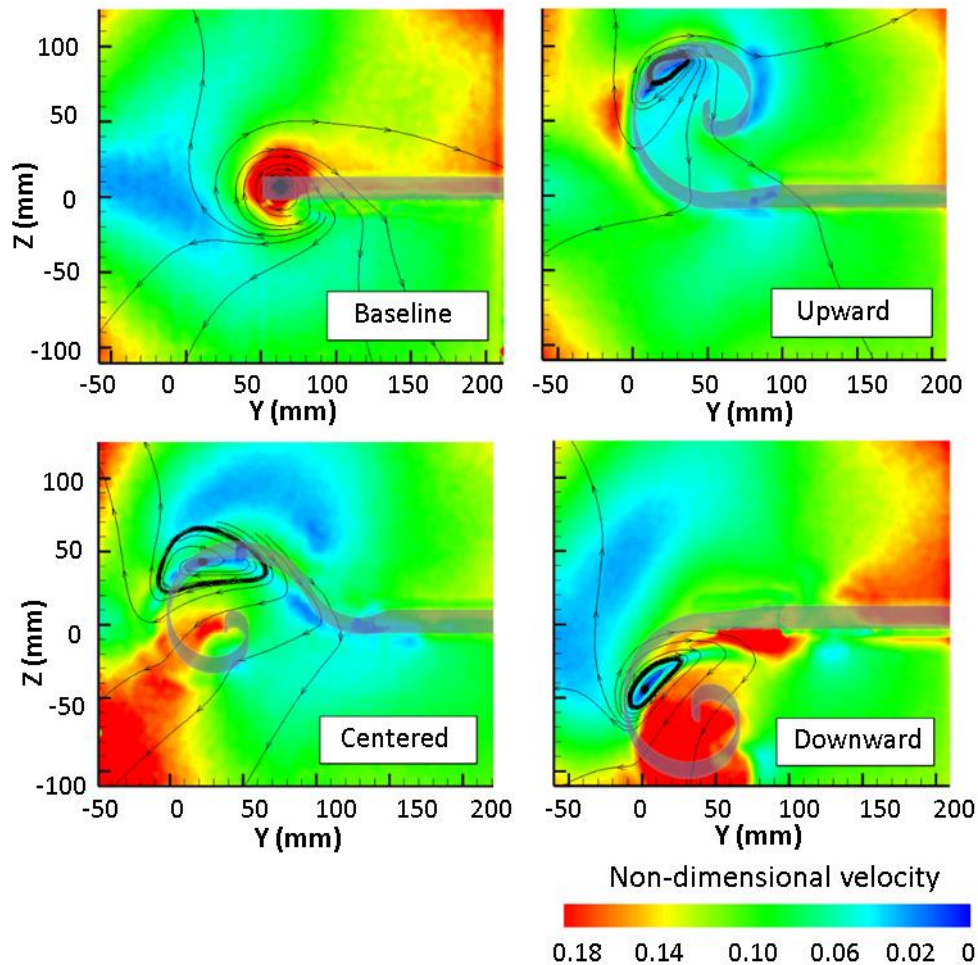


Fig. 8 Comparison of wingtip vortex transversal maps for $\alpha = 5^\circ$.

Figure 9 shows the non-dimensional vertical velocity maps obtained by PIV at the angle of attack of 18° for the four winglet configurations. In the cases where wingtip devices are tested, a noticeable reduction in velocity magnitude compared to the baseline case is observed with the upward CVG configuration demonstrating the most significant reduction.

Downstream of the vortex formation, the turbulent flow separates into two distinct regions: one with positive vertical velocities and the other with negative vertical velocities. This separation results in a larger spatial extent of the vortex and a more complex central location.

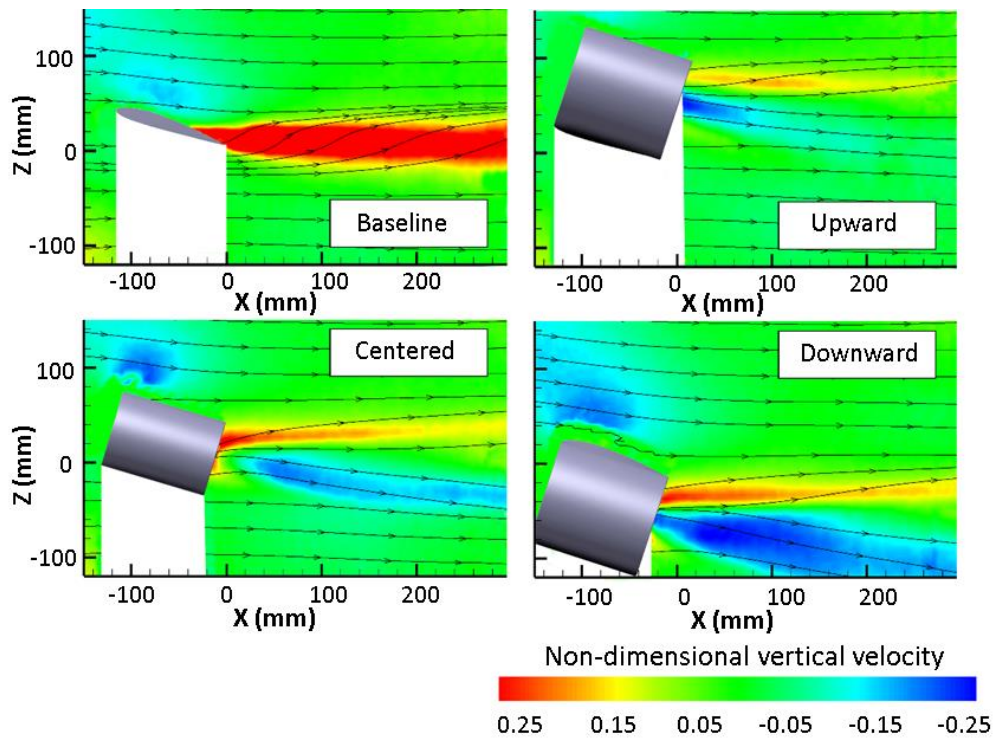


Fig. 9 Comparison of wingtip vortex lateral maps for $\alpha = 18^\circ$.

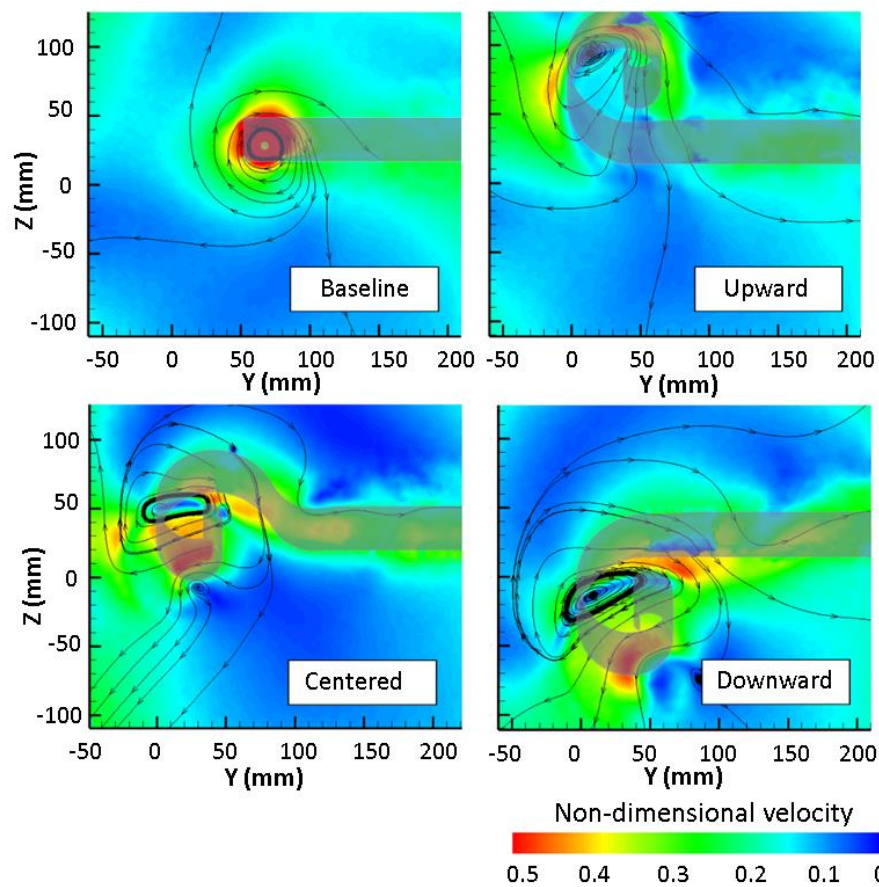


Fig. 10 Comparison of wingtip vortex transversal maps for $\alpha = 18^\circ$.



As illustrated in Figure 10, the cross-sectional maps show that the stream adapts to the shape of the flow control devices. In the earlier-mentioned cases, where the spiral's rotation direction is "Counterclockwise" and opposes the vortex formation's rotation, a secondary counter-rotating vortex emerges.

Table 2 presents the vortex centers for each wingtip configuration and for both angles of attack. The data clearly show that the location of the vortex core is significantly influenced by the shape and position of the Columnar Vortex Generator's spiral.

Table.2 Location of the vortex core in all wing configurations.

Configuration	Coordinates at $\alpha = 5^\circ$	Coordinates at $\alpha = 18^\circ$
Baseline	Y : 13.3 mm; Z: 8.5 mm	Y : 17.4 mm; Z: 28.7mm
Upward CVG	Y : 20.5 mm; Z: 84.9 mm	Y : 13.5 mm; Z: 93.5 mm
Centered CVG	Y : 22.5 mm; Z: 42.9 mm	Y : 13.6 mm; Z: 52.6 mm
Downward CVG	Y : 22.5 mm; Z: -44.3 mm	Y : 8.9 mm; Z: -13.5 mm

Final Selection of the Optimal Columnar Vortex Generator's configuration

A comparative analysis of the non-dimensional maximum vertical velocity magnitude (\bar{V}_{max}/U_∞) was conducted for each flight condition. From the vertical velocity $v(x, z)$ data collected on the lateral PIV planes positioned 1 cm from the tip of the wingtip, the velocity magnitude (\bar{V}) was obtained for each winglet configuration. Figure 11 shows the percentage variation of the non-dimensional maximum vertical velocity magnitude for all winglet configurations for the angle of attack of 5° .

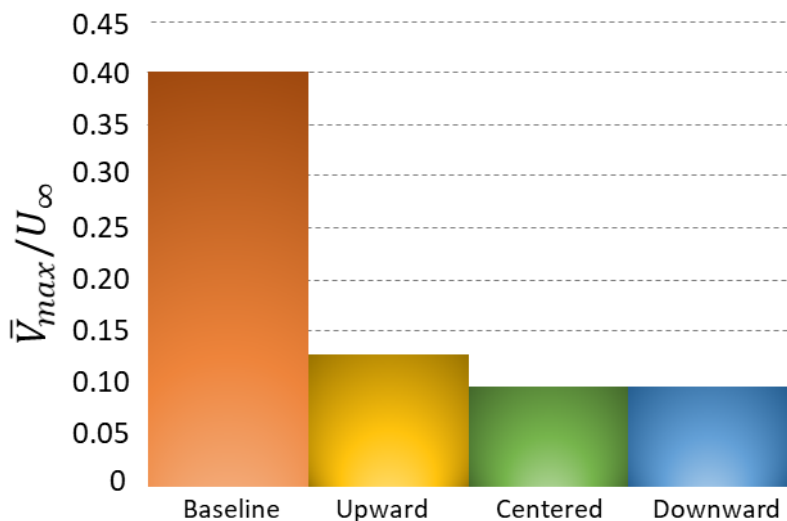


Fig. 11 Non-dimensional maximum vertical velocity magnitude for $\alpha = 5^\circ$.

It can be observed that all winglet configurations result in a significant reduction in velocity compared to the baseline case. The upward CVG reduces the induced velocity by up to 68 % compared to the baseline configuration, while the maximum velocity reduction, around 75 %, is achieved in the other two configurations (upward CVG and centered CVG).

Figure 12 illustrates the percentage variation in the non-dimensional maximum velocity magnitude for all winglet configurations at an angle of attack of 18°. Under this flight condition, the upward CVG configuration achieves the greatest velocity reduction, approximately 75 % compared to the baseline case. The other two configurations (centered CVG and upward CVG) can reduce the velocity by up to 69 % compared to the baseline configuration.

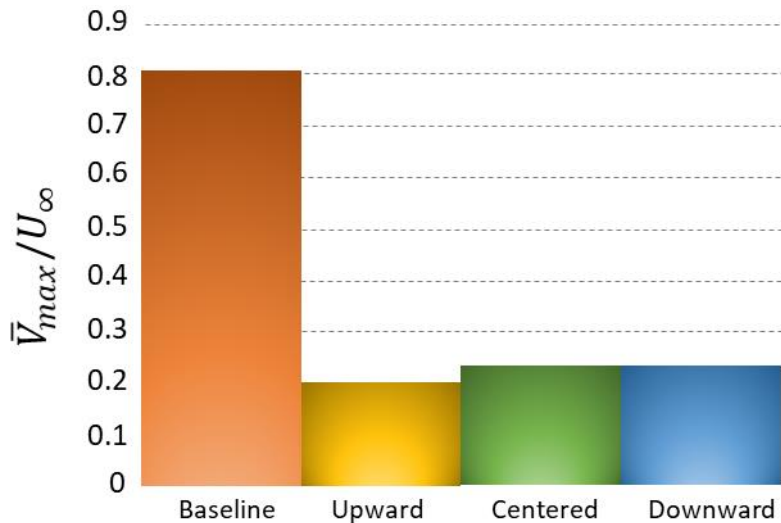


Fig. 12 Non-dimensional maximum vertical velocity magnitude for $\alpha = 18^\circ$.

5. Conclusions

Three wingtip devices, inspired by the characteristic spiral of the Columnar Vortex Generator (CVG) flow control device, have been designed. An aerodynamic flow investigation around the wingtip vortex was conducted in a wind tunnel, utilizing non-intrusive full-field measurements acquired through Particle Image Velocimetry (PIV) to compare velocity maps among the studied cases.

It was observed that all devices reduce the velocity induced by the wingtip vortex in the baseline configuration. Notably, the downward CVG and centered CVG devices exhibited superior performance at the angle of attack of 5°, while at the angle of attack of 18°, the benefit in velocity reduction was less pronounced. At the angle of attack of 18°, the upward CVG configuration demonstrated a greater reduction in induced velocity compared to the other two configurations. Moreover, the experimental data showed that the location of the center of the spiral was very influential in the flow direction.



Finally, this study successfully characterizes the performance of the flow control devices (Columnar Vortex Generators - CVGs) implemented as wingtip devices on a wing.

References

- [1] Stöcker C., Bennett R., Nex F., Gerke M. & Zevenbergen J. “Review of the Current State of UAV Regulations”, MDPI, 2017.
- [2] Guerrero J. E., Maestro D. & Bottaro A. “Biomimetic spiroid winglets for lift and drag control”, Elsevier, 2012.
- [3] B. Makgantai, N. Subaschandar and Jamisola Jr, R. S., “Design Optimization of Wingtip Devices to Reduce Induced Drag on Fixed-Wings”, International Conference on Unmanned Aircraft Systems (ICUAS), Athens, 2021.
- [4] Cosin R., Catalano F. M., Correa L. G. N. & Entz R. M. U. “Aerodynamic analysis of multi-winglets for low speed aircraft”, 27th International Congress of the Aeronautical Sciences, 2010.
- [5] Bardera-Mora R., Barcala-Montejano M., Rodríguez-Sevillano A. & Nova-Trigueros J. “Passive flow control over the ski-jump of aircraft carriers”, Ocean Eng., 1997.
- [6] Jansen, D., “Passive Flow Separation Control on an Airfoil-Flap Model: The Effect of Cylinders and Vortex Generators”, Aerospace Engineering, 2012.
- [7] A. Murtaza, Dr. K. Parvez, H. Shahid, Y. Mehmood. “Design and computational fluid dynamic analysis of spiroid winglet to study its effects on aircraft performance”, International Research Journal of Engineering and Technology, 2017.
- [8] D. Adnan Abd, Dr. A. H. Ali. “Aerodynamic Characteristics Comparison between Spiroid and Blended Winglets”, Journal of Engineering, 2020.
- [9] McAlister K. W. & Takahashi R. K. “NACA 0015 Wing Pressure and Trailing Vortex Measurements”, NASA Technical Paper, 1991.
- [10] Bardera R., Barcala-Montejano M., Rodriguez-Sevillano A. & Matías-García J.C. “Passive flow control over the roof of buildings by using columnar vortex generator”, International Research Journal of Engineering and Technology, 2017
- [11] Raffel M., Willert C. E., Wereley S. T. & Kompenhans J. “Particle Image Velocimetry: A Practical Guide”, 2007.
- [12] S. Mostafa, S. Bose, A. Nair, M. A. Raheem, T. Majeed, A. Mohammed, Y. Kim. “A parametric investigation of non-circular spiroid winglets”, Department of Aeronautical Engineering, Emirates Aviation College, Dubai, 2014.



Copyright Statement

The authors confirm that they, and/or their company or organization, hold copyright on all of the original material included in this paper. The authors also confirm that they have obtained permission, from the copyright holder of any third party material included in this paper, to publish it as part of their paper. The authors confirm that they give permission, or have obtained permission from the copyright holder of this paper, for the publication and distribution of this paper as part of the ICAS proceedings or as individual off-prints from the proceedings.